Measurement System for the Temperature Behavior Investigation of Phase Change Materials

Maria Natalia R. Dimaano
Research Center for the Natural Sciences/Faculty of Engineering
University of Santo Tomas, España, Manila 1008 Philippines
e-mail: dimaano@nsclub.net

Takayuki Watanabe
Research Laboratory for Nuclear Reactors
Tokyo Institute of Technology, 2-12-1 O-okayama
Meguro-ku, Tokyo, 152-8550 Japan
Email: watanabe@nr.titech.ac.jp

ABSTRACT

The performance of the temperature measurement system using different phase change material (PCM) mixtures for low temperature thermal energy storage application was characterized. Temperature measurements at varied height positions exhibited adequate radial temperature behavior on both melting and solidification processes with different PCM mixtures. The temperature history projected from the measurement elucidated the characteristic thermal performance of different PCM mixtures. The evaluation of the total amount of heat charged and discharged in the PCM suggested an improvement on the probe set-up support to come up with a better efficiency of the whole storage system set-up.

Keywords: phase change material, temperature measurement, thermal energy storage

1. INTRODUCTION

The dramatic increase in energy costs compounded by the uncertainty about future fuel supply sources led to an innovative approach to provide the necessary cool through the low-temperature thermal energy storage system. Energy is stored in frozen phase change materials (PCMs) during off peak periods and released the next day for air conditioning or process cooling [Dudley, et.al.]. Although PCMs have been identified since the early 1980s, they are still considered “new kids on the cool storage block”.

The efficiency of PCMs depends on its ability to store the needed amount of energy and consequently change the temperature of an adjacent space unit. The knowledge of the thermal characteristics of PCMs involves careful execution and evaluation of the melting and solidification experiments. This requires a sensitive method for temperature measurement during phase change.

In the course of our study of the mixture of the capric acid and lauric acid (C-L acid) as PCM for low-temperature thermal energy storage [Dimaano, et.al.], a temperature measurement system has been fabricated. It is then the objective of this study to confirm the efficiency and characterize the adequacy of the temperature measurement system using different PCMs and their mixture.

2. MATERIALS AND METHODS

2.1. Materials

The PCMs used were the C-L acid, primarily composed of 65% capric acid and 35% lauric acid by mole, pentadecane, and the mixtures of C-L acid and pentadecane (CL:P) in the respective combinations of 90:10, 70:30, and 50:50, by volume. Tokyo Chemicals Inc.

manufactured the three chemicals with purity of 98% for both capric and lauric acids and 99% for pentadecane.

2.2. Temperature Probe

Base metal Type K chromel and alumel wires each having 0.28mm diameter was joined in one end by gas welding. The probe junction beads formed diameters ranging from 0.6 to 0.9 mm. Accuracy of the thermocouples were tested using ice point 0°C as the reference temperature and water at different controlled temperatures. Calibration of thermocouples was achieved comparing values with established Type K standards. Simultaneously, the thermocouples were further subjected to heating (0→45°C) and then to cooling (45→0°C) processes. Thermocouples that exhibited similar temperature readings were chosen for the temperature probe sensor set-up.

2.3. Temperature Measurement System

Ten thermocouples were arranged as presented in Fig. 1 to determine the radial temperature distribution in the PCM mixture throughout the melting and solidification processes. The thermocouples were held in 2 rectangular acrylic slabs, with each slab having ten holes positioned as indicated in Fig. 1.

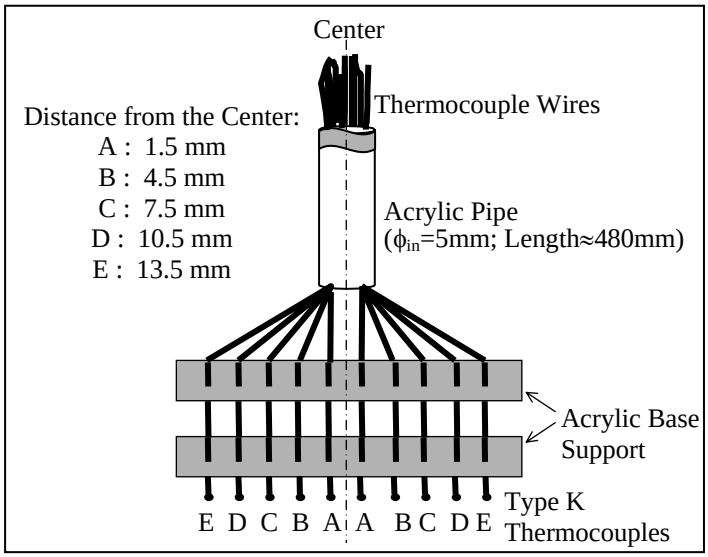

Fig. 1. Chromel-Alumel (Type K) thermocouple probe set-up.

This probe sensor set-up was placed inside the copper tube encapsulating the PCM mixture. The set-up was also varied at different height positions of 0, 100, 200, and 300 mm from the base of the copper tube. The thermocouples were connected to a computer based electronic data acquisition system using the multiple converter Yew Model 3081 Hybrid Recorder. This converter performed a time division multiplexing operation between the different sensor inputs providing simultaneous readings every 6 seconds of time interval. Each channel was sequentially connected to the analogue to digital converter itself controlled by inputs from the data processor integrated in the designed computer program.

Water served as the heat transfer fluid and was kept at average temperatures of 8.3 °C for pure C-L acid and 5.5 °C for all CL:P combinations at a flow rate of 2.51 x 10^{-5} m^3/s during the solidification process. During melting, water was maintained at average temperatures of 34.5 °C for C-L acid and 35.0 °C for all CL:P combinations at a flow rate of 1.67x10^{-5} m^3/s. Water entered the bottom and exited at the top of the storage capsule on both melting and solidification processes.

3. RESULTS AND DISCUSSION

3.1. Radial Temperature Profile

Figure 2 shows a representative profile during a melting process. The melting band represents the phase transition region establishing the melting range evaluated from 90% of the total height of the melting curve of the PCM obtained from the Differential Scanning Calorimetry (DSC) analysis. The total height is the vertical measurement of the PCM thermal event from its baseline to its melting peak. Below the melting band is the solid phase and above the melting band is the liquid phase. The phase transition activity occurs within the melting band.

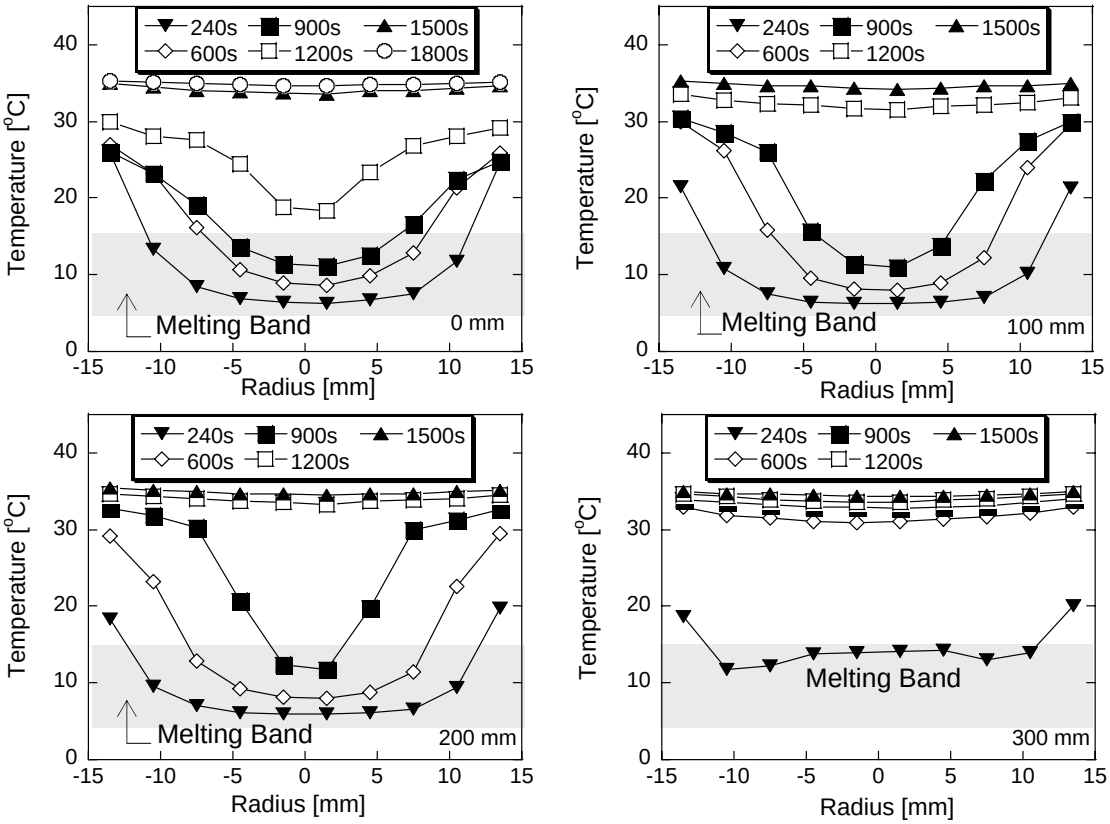

Fig. 2. Temperature measurements at different radial and axial positions represented by 70-30 CL:P at 35.1 ^{o}C and 1.67 x 10^{-5} m^3/s of inlet water temperature.

Well-defined concave temperature curves indicate higher temperatures bound on the liquid region. It signifies an instantaneous melt on the outermost radius, while temperature lags on the inner radii. The sharpness of the peaks diminishes at longer times until the radial temperature distribution finally flattens. This indicates the attainment of complete melt by the PCM.

Instantaneous symmetry in the radial temperature distribution is maintained during the smooth deliquescent stage of the PCM during melting. Non-symmetry are also observed revealing the spontaneous hysteresis or delay in the probe measurement. This is a characteristic feature that is within the allowable variation in the measurement system and does not substantially interfere with the heat transfer mechanism of the storage system.

3.2. Axial Temperature Behavior

As charging proceeds, the temperature in the inner radii rises correspondingly in the succeeding higher layers of the PCM. The highest PCM layer tends to melt quickly as it occupies the upper temperature limit of the melting band. This is shown by the radial

temperature profile at 240s in the 300 mm probe height position. At longer charging time, the flattening of the radial temperature distribution becomes relatively faster at higher height positions. Melting proceeds from the top to the bottom of the storage capsule.

Since water flows from the bottom of the storage capsule, the lowest layer starts solidifying first on the initial solidification stage. Once the solid has established, solidification develops on the succeeding higher layers of the PCM.

3.3. Temperature History

Figure 3 shows the typical melting and solidification temperature histories of PCMs. It demonstrates the variation of water inlet and outlet temperatures as well as the radial temperatures of the PCM with time. The heat energy contained/required in the PCM is maximally charged/discharged by water during the early stage of the melting/solidification process. In general, temperatures at varying height and radial positions indicate a generally minute lowering from the outer radius inward during solidification and a normal increase outward during melting. Melting proceeds fast from the outer radius and then gradually slows toward the inner radii. Similar behavior in the decreasing temperature trend is observed for the solidification process.

From the temperature history, the melting time of the PCM is estimated from the beginning of the process until the innermost radius attains the higher temperature limit in the melting band. The solidification time is taken from the initial time until the innermost radius reaches the lower melting band limit. Figure 4 indicates that complete solidification of the 70:30 CL:P was not attained. The experiment stopped at 5000s while the solidification process had not yet terminated. The temperature setting of 5.1 ^{o}C in water was insufficiently higher than the PCM's lower melting band limit. Thus, the radial temperatures, as well as the water temperatures, had not reached the lower melting band limit.

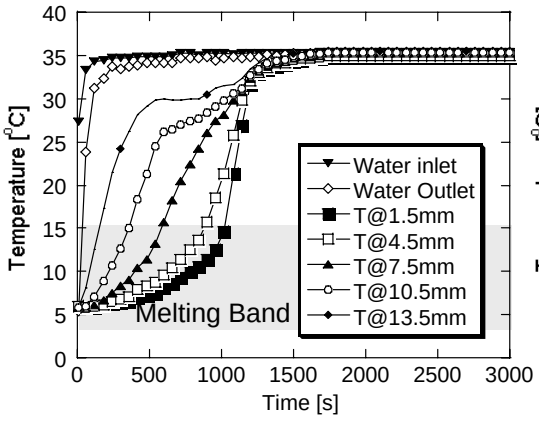

Fig. 3. 70:30 CL:P melting at 100 mm probe height setting at 35.1 ^{o}C and 1.67 x 10^{-5} m^3/s of inlet water.

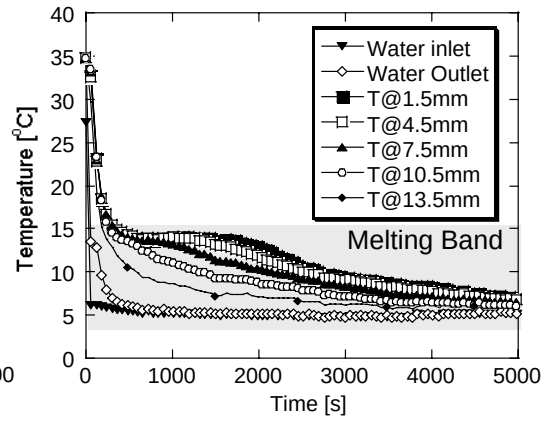

Fig. 4. 70:30 CL:P solidification at 100 mm probe height setting at 5.1 ^{o}C and 2.51 x 10^{-5} m^3/s of inlet water.

3.4. Effectiveness to Heat Transfer Investigation

Further test to examine the efficiency of the measurement system was conducted by evaluating the total amount of heat stored in the PCM measured from its radial temperature distribution at different height positions. The total amount of heat charged and discharged during melting and solidification were estimated from the solid and liquid sensible heats prior and after phase transition and the heat energy accounted from the latent heat and the sensible heat derived from the large melting band of the PCM during phase transition. The sensible heats (J_{SH}) were computed, integrating implicitly with time the following relation

$$J_{SH} = \int\int \rho \, Cp \, dT \, dV \qquad (1)$$

The energy stored due to latent heat (J_{LH}) was determined considering the immobile layer of either the liquid or solid material expressed in terms of the melt/solid fraction (α) that continually grew as the PCM gave up its heat of fusion as

$$J_{LH} = \int\int \rho\, L\, d\alpha\, dV \tag{2}$$

Figures 5 and 6 show the integrated heat charged and discharged in a representative PCM at different probe height settings during melting and solidification, respectively. With a representative 0.2 kg of PCM sample used in the study, the smooth curve that have ensued along the latent heat region and finally leveling horizontally along the liquid phase region conformed with the theoretical total amount of heat charged equivalent to ~39 kJ. Discrepancies in the final charged energy in different probe height positions particularly in solidification are within the agreeable deviation range (7%). The initial PCM solidification temperature of about 8.7 ^{o}C caused a 5.7 ^{o}C difference marking an insufficient response in the sensible heats discharged equivalent to ~2.5 kJ deficiency during solidification.

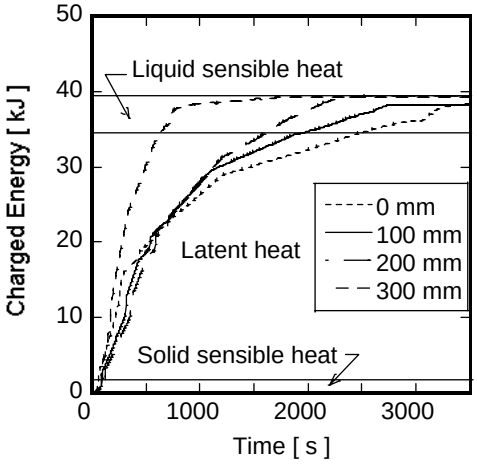

Fig. 5. Total heat stored in pure C-L acid during melting with initial temp. of 8.3 ^{o}C and final temperature of 34.4 ^{o}C.

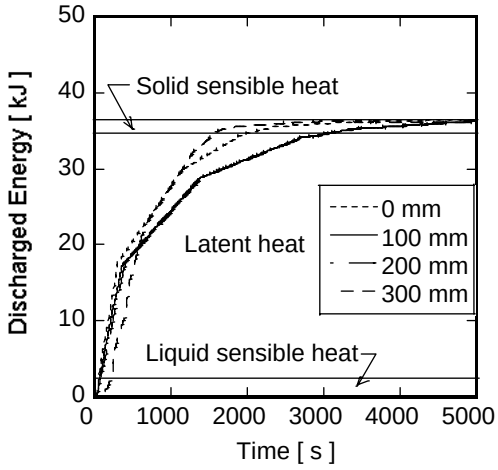

Fig. 6. Total heat stored in pure C-L acid during solidification with initial temp. of 28.7 ^{o}C and final temperature of 8.3 ^{o}C.

A distinct behavior during the charging and discharging of heat by the PCM (Figs. 5 and 6) was observed in different probe height positions. This may be explained by two factors. One deterring factor is the probe set-up positioned midway along the PCM column. The acrylic bases that support the probes tend to hinder an effective convection to take place during melting. This addresses to the eventual modification of the PCM probe set-up. Another factor is that phase transition itself is complicated by the existence of both conduction and convection modes of heat transfer. Natural convection governs during the melting process. However, the existence of solids that drops down the column combined with the natural convection during the PCM phase transition cause the impairment of heat transfer along the PCM column.

Similar behavior was demonstrated in the PCM during solidification but with lesser discrepancy due to a more stable heat transfer governed by conduction. As solidification proceeded from the bottom of the storage capsule upward, the lowest layer discharged heat ahead followed by the next higher layers of the PCM. This is explained by the greater temperature difference in the lower layer and smaller in the higher layer.

Figure 7 shows the melting times of PCMs depicting their melting rates. The upper limit of the melting band (Table 1) has a considerable effect on the melting time. Although a higher latent heat furnishes greater heat capacity, it leads to a longer melting time. Shorter melting time provides a faster heat transfer rate alleviating the total storage system cost for industrial application.

Since the 50:50 CL:P has the lowest temperature in its upper melting band among the other PCMs, it represented the shortest melting time, consequently followed by pentadecane, 70:30 CL:P, 90:10 CL:P and the C-L acid. The relative decrease in the melting time as it proceeds up the higher axial position indicates that melting indeed proceeds from the highest

layer down the column. Inconsistencies in the melting times at the highest axial position mark the instability tolerably influenced by natural convection.

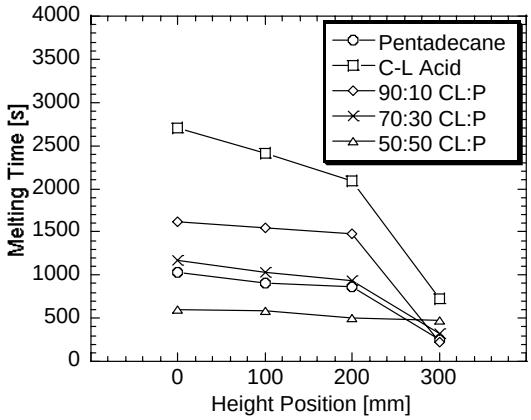

Fig. 7. Melting times of different PCMs in different probe height settings with 34.8 ^{o}C and 1.67 x 10^{-5} m^3/s of inlet water.

Table 1. Melting characteristics information obtained from DSC analysis.

Phase Change Material	Melting Band [^{o}C]		Melting Peak [^{o}C]		Latent Heat
	Lower Limit	Upper Limit	First Peak	Second Peak	[kJ/kg]
C-L Acid	16.0	23.0	22.6		148.0
90:10 CL:P	3.7	15.8	6.3	16.4	154.7
70:30 CL:P	3.9	15.7	6.4	14.5	157.5
50:50 CL:P	4.0	12.2	6.7	12.5	162.4
Pentadecane	7.6	13.3	11.5		168.0

5. CONCLUSION

The radial and axial behavior of the temperature measurement system had been characterized. The total amount of heat charged and discharged in the PCM measured from the radial temperature distribution conformed to the thermal energy that it should generate. However, inconsistencies in the results of the axial thermal performance evaluation addressed the need to make partial changes on the probe set-up. An adjustment modification on the probe support is now considered for future work to meet the adequacy of the PCM temperature measurement for thermal energy storage system.

NOMENCLATURE

Cp	specific heat of PCM [kJ/kg.K]	L	latent heat [kJ/kg]
dt	differential time [s]	T	PCM radial temperature [K]
dV	differential volume of PCM [m^3]	α	melting or solidification fraction
J	Total heat energy stored [kJ]	ρ	density [kg/m^3]

REFERENCES

Dimaano, M. N. R. and Escoto, A. (1998). ***Preliminary Assessment of a Mixture of Capric Acid and Lauric Acids as Phase Change Materials for Thermal Energy Storage.*** Energy-The International Journal **23 (5),** 421-427.

Dimaano, M. N. R. and Watanabe, T. (1997). ***Measure of the Radial Temperature Behavior of Pentadecane: A Preliminary Study***, Bulletin of INCOCSAT, T.I.T., 92-97.

Dudley, J. C. and Freedman, S. I. (1975). ***Economics of Operating Energy Storage Air Conditioning Systems with Reduced Peak Power Demand***, ASHRAE Trans. **81**, Part I.